

# **Computational Sciences and Engineering**



journal homepage: https://cse.guilan.ac.ir/

# Analyzing bifurcation, stability and soliton solutions of Wang equation with a multiplicative white noise using Hamiltonian and Jacobian techniques

Mostafa Eslami <sup>a,\*</sup>, Anis Esmaeily <sup>a</sup>, Hamood Ur Rehman <sup>b</sup>

#### ARTICLE INFO

Article history: Received 9 February 2025 Received in revised form 9 April 2025 Accepted 19 April 2025 Available online 19 April 2025

Keywords:
Wang equation
Analyzing bifurcation
Chaotic behaviors
Sensitivity analyzing
Stability of the critical points

#### ABSTRACT

The nonlinear Schrödinger equation (NLSE) appears in many fields like quantum mechanics, optical fiber communications, plasma physics, and superfluid dynamics. In this context, we focused on the extended (3 + 1)- dimensional stochastic NLSE. Specifically, we will explore these equations under the influence of multiplicative noise in the Itô framework. We apply the Sardar sub-equation method to investigate the exact solutions of the extended (3+1) - dimensional stochastic nonlinear Schrodinger equation under the influence of multiplicative noise. This method simplifies this nonlinear equation and derive the soliton-like, periodic, bright, dark and singular solutions, which are crucial for understanding wave propagation and stability in various physical systems. In this framework, bifurcation analysis allows us to explore how the system transitions at critical points or parameter thresholds. Chaotic behaviors are further examined by adding the external periodic functions. We can characterize regions where chaotic motion emerges, offering insights into unpredictable and turbulent behaviors that are common in plasma physics and optical fibers. Sensitivity analysis helps quantify how variations in system parameters influence the dynamics of the equation. By linearizing the system near equilibrium solutions, the stability of critical points is also investigated. Moreover, we present the behavior of these solutions graphically. By plotting the solutions obtained from the Sardar subequation method, we can observe the formation of solitons. Graphical illustrations of bifurcations, chaotic regimes and stability regions to enhance both qualitative and quantitative analysis of the system.

E-mail addresses: mostafa.eslami@umz.ac.ir (M. Eslami)

<sup>&</sup>lt;sup>a</sup> Department of Applied Mathematics, Faculty of Mathematical Sciences, University of Mazandaran, Babolsar, Iran

<sup>&</sup>lt;sup>b</sup> Department of Mathematics, University of Okara, Okara, Pakistan

<sup>\*</sup> Corresponding author.

#### 1. Introduction

Nonlinear partial differential equations (NLPDEs) are a significant tool in mathematical modeling to provide an effective framework for studying processes that evolve over time and change across spatial dimensions [1]. NLPDEs are utilized across numerous scientific and engineering disciplines, including fluid dynamics, heat transfer, quantum mechanics, and wave propagation. To tackle these complex problems, a mix of numerical and analytical approaches, such as finite element methods, finite difference, Fourier analysis and separation of variables, is often employed [2,3]. These techniques enable the study of complex systems where exact analytical solutions are difficult or impossible to derive. As a result, an understanding of PDE theory along its applications is important for professionals and researchers in various fields, empowering them to explore and solve real-world problems in both natural and engineered systems [4,5].

Stochastic partial differential equations (SPDEs) provide a mathematical framework for making systems influenced by random variations and are widely used in different fields such as physics, economics, biology, and engineering, where uncertainty has a significant role [6,7]. Unlike other differential equations, SDEs have stochastic processes, making the evolution of the system more unpredictable. This unpredictability can come from different sources such as economic fluctuations, biological inefficiencies or environmental noise, SDEs analyze how both deterministic and random factors interact to influence system behavior. A critical aspect of SDEs is Itô calculus, which provides the tools to work with stochastic integrals and differentials, along with the concepts of strong and weak solutions that describe different scenarios of system behavior. Understanding the mathematical properties of SDEs with their practical applications, sets the stage for deeper investigation of this area of mathematics [8,9]. The Wiener process is a key mathematical model for presenting random fluctuations to offer insights into the variability and behavior of systems across fields like engineering, finance and physics. Its properties, such as self-similarity and its Gaussian distribution, make it valuable for modeling a variety of stochastic phenomena. The Wiener process is important for studying how randomness influences system dynamics and is foundational for predicting and understanding variations in many applications. The Wiener process is crucial for investigating the role of randomness in improving system performance and optimizing processes [10-13]. The discovery of optical solitons, their selfreinforcing nature and stability have led to many breakthroughs and performance improvements over the last few decades [14-16]. Several sophisticated mathematical approaches have been developed to describe and manipulate solitons, including the sine-cosine, sinh-cosh methods, Kudryashov method, advanced forms like the Hirota bilinear method and many others. Over time, different types of solitons have been identified, including dispersion-managed solitons, cubicquartic solitons and non-Kerr solitons [17-21]. These developments have also uncovered new phenomena like unique forms of self-phase modulation. The exploration of solitons has spurred a steady stream of innovative ideas and continuously enhancing our understanding and application of these waves. Many governing models are used for studying soliton propagation in optical fibers. A recent innovation in this area involves combining established models to create new approaches that can more effectively manage soliton dynamics over intercontinental distances. One such model, which has gained attention in nonlinear fiber optics, integrates three well-known equations: the nonlinear Schrödinger equation (NLSE), the Sasa-Satsuma equation (SSE) and the Lakshmanan-Porsezian-Daniel (LPD) model. A lot of research has been conducted on this combined model, exploring various aspects in detail. The concatenated model has been analyzed using the Painlevé approach, and optical solitons have been derived within its framework. These studies have examined soliton behavior in birefringent fibers under this model, and the incorporation of power-law nonlinearities has also been explored. The NLSE is widely recognized as a mathematical equation used to explain the behavior of slow wave packets in many nonlinear wave systems and has significant applications in fields such as condensed matter physics, nonlinear optics, and other areas of physical science [21-23]. As scientific developments continue and research deepens, more complex models are required to accurately represent real-world nonlinear phenomena. Consequently, the standard NLSE has been expanded to include versions with variable coefficients, multi-dimensional forms, non-local effects, higher-order terms, fractional orders, and even combinations of these extensions. Recently, Wang explored a novel (3+1)-dimensional sine-Gordon and sinh-Gordon equation derived from an extended (3+1)dimensional zero curvature equation [24]. In this paper, we aim to derive a extended (3+1)dimensional Schrödinger equation in the sense of noise term [25]. We applied Sardar sub-equation method to derive the soliton solution of the equation in the form of dark, bright, singular, and periodic-singular solutions [26]. The main objective of this study is to thoroughly explore the dynamics described by the extended (3+1)-dimensional stochastic NLSE. The process starts by using the Galilean transformation to lead the derivation of the associated dynamical system. The Galilean transformation facilitates the transition from a moving reference frame to a stationary one by converting NLPDEs into ODEs. This permits the spatial derivative terms in the original NLPDEs to be expressed as time derivatives and simplifying the mathematical process to enable easier solutions of the obtained ODE system.

The paper also applies the established theory of planar dynamical systems to perform a detailed bifurcation analysis, which expose the complex behaviors exhibited by the system. This analysis delves into the investigation of chaotic dynamics in the model and to achieve this, an external term is added into the dynamical system. The investigation of chaotic behavior is analyzed with the aid 2D and 3D phase portraits which provide a thorough understanding of the system's intricate dynamics [28,29]. Furthermore, the Runge–Kutta method is employed to conduct a sensitivity analysis of the system which ensure the stability of the solutions against small perturbations in initial conditions. By introducing slight variations and evaluating their effects on stability, the reliability and consistency of the derived solutions are validated. By linearizing the system near equilibrium solutions, the stability of critical points is also investigated. Notably, this study highlights its originality and emphasizing that such an investigation has not previously been conducted for the system in question.

#### 2. Mathematical model

In this work, the extended (3 + 1)-dimensional stochastic nonlinear Schrodinger equation (NLSE) to be considered is given by [25]

$$iu_t - \left(a_1 u_{xx} + a_2 u_{yy} + a_3 u_{zz} + 2a_4 u_{xy} - 2a_5 u_{xz} - 2a_6 u_{yz}\right) + b|u|^2 u + \sigma u \frac{dW(t)}{dt} = 0,$$
 (1)

These coefficients  $a_l$ , (l=1,2,3,4,5,6), b are constants. The role of  $\sigma$  is to signify the coefficient of noise strength, while W(t) corresponds to the standard Wiener process, and  $\frac{dW(t)}{dt}$  expresses the white noise. When  $\sigma=0$ , we have the Wang equation [24]. If  $a_1=-a$ ,  $\sigma=a_2=a_3=a_4=a_5=a_6=0$ , we give the NLSE [30].

#### 3. Mathematical analysis

To kick off, the following hypothesis is picked [25,31]

$$u(x, y, z, t) = P(\xi)e^{i\Phi(x, y, z, t)}, \tag{2}$$

Where  $P(\xi)$  represent the shape of the pulse and

$$\xi = B_1 x + B_2 y + B_3 z - Vt \,, \tag{3}$$

Where

$$V = 2B_1(a_1\kappa_1 + a_4\kappa_2 - a_5\kappa_3) + 2B_2(a_2\kappa_2 + a_4\kappa_1 - a_6\kappa_3) + 2B_3(a_3\kappa_3 - a_5\kappa_1 - a_6\kappa_2), \tag{4}$$

and the phase component is defined as

$$\Phi(x, y, z, t) = -\kappa_1 x - \kappa_2 y - \kappa_3 z - \sigma^2 t + \sigma W(t) + \omega t + \theta,$$
(5)

Here,  $\kappa_1$ ,  $\kappa_2$ ,  $\kappa_3$ , are the soliton frequency,  $\omega$  is the wave number, while  $\sigma$  corresponds to the noise coefficient and  $\theta$  is the phase constant. Substituting Eqs. (2),(3),(4) and (5) into Eq.(1) and decomposing into real and imaginary parts, give

$$-LP'' - (\omega - \sigma^2 - S)P + bP^3 = 0, (6)$$

Where

$$L = a_1 B_1^2 + a_2 B_2^2 + a_3 B_3^2 + 2a_4 B_1 B_2 - 2a_5 B_1 B_3 - 2a_6 B_2 B_3,$$
 (7)

And

$$S = a_1 \kappa_1^2 + a_2 \kappa_2^2 + a_3 \kappa_3^2 + 2a_4 \kappa_1 \kappa_2 - 2a_5 \kappa_1 \kappa_3 - 2a_6 \kappa_2 \kappa_3.$$
(8)

#### The Sardar- sub-equation procedure

The Sardar –Sub-equation method is very effective to derive the exact solution of different (NLSE). This section will describe the short description about this method [26,27]. In Eq. (6), balancing  $P^3$  ( $\xi$ ) with  $P''(\xi)$  yield N=1. The solution is expressed in the following structure:

$$P = g_0 + g_1 \pi(\xi), \tag{9}$$

That  $\pi(\xi)$  satisfies the following equation:

$$\pi'(\xi) = \sqrt{\kappa + \beta \pi(\xi)^2 + \pi(\xi)^4},\tag{10}$$

Inserting Eq. (9) together with Eq. (10) into Eq. (6), we get a system of algebraic equations. Solving these equations together yields the following:

$$eq1 = bg_1^3 - 2Lg_1 = 0,$$

$$eq2 = 3bg_1^2g_0 = 0,$$

$$eq3 = -2\left(\frac{-3bg_0^2}{2} + \frac{L\beta}{2} - \frac{\sigma^2}{2} - \frac{S}{2} + \frac{\omega}{2}\right)g_1 = 0,$$

$$eq4 = g_0(bg_0^2 + \sigma^2 + S - \omega) = 0.$$
(11)

Solving the resulting system, we get

$$g_0 = 0, g_1 = \sqrt{\frac{2L}{b}}, \beta = \frac{\sigma^2 + S - \omega}{L},$$

$$g_0 = 0, g_1 = -\sqrt{\frac{2L}{b}}, \beta = \frac{\sigma^2 + S - \omega}{L}.$$
(12)

By using Eqs. (3), (9), (10), and (12), solutions of Eq. (6) is obtained,

**Case I**: If  $\beta > 0$ , and  $\kappa = 0$ , afterward:

$$\begin{split} P_{1,1}^{\pm} &= \pm \sqrt{\frac{2L}{b}} \left( \sqrt{-fg\,\beta} \right) sech_{fg} \left( \sqrt{\beta}\,\xi \right), \\ q_{1,1}(x,y,z,t) &= \pm \sqrt{\frac{2L}{b}} \left( \sqrt{-fg\,\beta} \right) sech_{fg} \left( \sqrt{\beta}\,\xi \right) \times e^{i\left(-\kappa_1 x - \kappa_2 y - \kappa_3 z - \sigma^2 t + \sigma W(t) + \omega t + \theta\right)}, \end{split} \tag{13}$$

$$P_{1,2}^{\pm} = \pm \sqrt{\frac{2L}{b}} (\sqrt{fg \beta}) \operatorname{csch}_{fg} (\sqrt{\beta} \xi),$$

$$q_{1,2}(x, y, z, t) = \pm \sqrt{\frac{2L}{b}} (\sqrt{fg \beta}) \operatorname{csch}_{fg} (\sqrt{\beta} \xi) \times e^{i(-\kappa_1 x - \kappa_2 y - \kappa_3 z - \sigma^2 t + \sigma W(t) + \omega t + \theta)},$$

$$(14)$$

Where  $\xi = B_1 x + B_2 y + B_3 z - Vt$ ,  $\beta = \frac{\sigma^2 + S - \omega}{L}$ .

**Case II**: If  $\beta$  < 0, and  $\kappa$  = 0, afterward:

$$P_{1,3}^{\pm} = \pm \sqrt{\frac{2L}{b}} \sqrt{-fg \,\beta} \, sec_{fg} \left( \sqrt{-\beta} \,\xi \right),$$

$$q_{1,3}(x,y,z,t) = \pm \sqrt{\frac{2L}{b}} \sqrt{-fg \,\beta} \, sec_{fg} \left( \sqrt{-\beta} \,\xi \right) \times e^{i\left(-\kappa_1 x - \kappa_2 y - \kappa_3 z - \sigma^2 t + \sigma W(t) + \omega t + \theta\right)},$$

$$(15)$$

$$P_{1,4}^{\pm} = \pm \sqrt{\frac{2L}{b}} \sqrt{-fg \beta} \csc_{fg} \left( \sqrt{-\beta} \xi \right),$$

$$q_{1,4}(x,y,z,t) = \pm \sqrt{\frac{2L}{b}} \sqrt{-fg \beta} \csc_{fg} \left( \sqrt{-\beta} \xi \right) \times e^{i(-\kappa_1 x - \kappa_2 y - \kappa_3 z - \sigma^2 t + \sigma W(t) + \omega t + \theta)},$$

$$(16)$$

Where  $\xi = B_1 x + B_2 y + B_3 z - Vt$ ,  $\beta = \frac{\sigma^2 + S - \omega}{L}$ .

Case III: If  $\beta < 0$ , and  $\kappa = \frac{\beta^2}{4}$ , afterward:

$$P_{1,5}^{\pm} = \pm \sqrt{\frac{2L}{b}} \sqrt{\frac{-\beta}{2}} \tanh_{fg} \left( \sqrt{\frac{-\beta}{2}} \xi \right),$$

$$q_{1,5}(x, y, z, t) = \pm \sqrt{\frac{2L}{b}} \sqrt{\frac{-\beta}{2}} \tanh_{fg} \left( \sqrt{\frac{-\beta}{2}} \xi \right) \times e^{i(-\kappa_1 x - \kappa_2 y - \kappa_3 z - \sigma^2 t + \sigma W(t) + \omega t + \theta)},$$

$$(17)$$

$$P_{1,6}^{\pm} = \pm \sqrt{\frac{2L}{b}} \sqrt{\frac{-\beta}{2}} \coth_{fg} \left( \sqrt{\frac{-\beta}{2}} \xi \right),$$

$$q_{1,6}(x,y,z,t) = \pm \sqrt{\frac{2L}{b}} \sqrt{\frac{-\beta}{2}} \coth_{fg} \left( \sqrt{\frac{-\beta}{2}} \xi \right) \times e^{i(-\kappa_1 x - \kappa_2 y - \kappa_3 z - \sigma^2 t + \sigma W(t) + \omega t + \theta)},$$

$$(18)$$

$$P_{1,7}^{\pm} = \pm \sqrt{\frac{2L}{b}} \left( \sqrt{\frac{-\beta}{2}} \left( \tanh_{fg} \left( \sqrt{-2\beta} \, \xi \right) \pm \sqrt{fg} \, \operatorname{sech}_{fg} \left( \sqrt{-2\beta} \, \xi \right) \right) \right),$$

$$q_{1,7}(x, y, z, t) = \pm \sqrt{\frac{2L}{b}} \left( \sqrt{\frac{-\beta}{2}} \left( \tanh_{fg} \left( \sqrt{-2\beta} \, \xi \right) \pm \sqrt{fg} \, \operatorname{sech}_{fg} \left( \sqrt{-2\beta} \, \xi \right) \right) \right)$$

$$\times e^{i(-\kappa_1 x - \kappa_2 y - \kappa_3 z - \sigma^2 t + \sigma W(t) + \omega t + \theta)},$$

$$(19)$$

$$P_{1,8}^{\pm} = \pm \sqrt{\frac{2L}{b}} \left( \sqrt{\frac{-\beta}{2}} \left( \coth_{fg} \left( \sqrt{-2\beta} \, \xi \right) \pm \sqrt{fg} \, \operatorname{csch}_{fg} \left( \sqrt{-2\beta} \, \xi \right) \right) \right),$$

$$q_{1,8}(x,y,z,t) = \pm \sqrt{\frac{2L}{b}} \left( \sqrt{\frac{-\beta}{2}} \left( \coth_{fg} \left( \sqrt{-2\beta} \, \xi \right) \pm \sqrt{fg} \, \operatorname{csch}_{fg} \left( \sqrt{-2\beta} \, \xi \right) \right) \right)$$

$$\times e^{i(-\kappa_1 x - \kappa_2 y - \kappa_3 z - \sigma^2 t + \sigma W(t) + \omega t + \theta)},$$
(20)

$$P_{1,9}^{\pm} = \pm \sqrt{\frac{2L}{b}} \left( \sqrt{\frac{-\beta}{8}} \left( \tanh_{fg} \left( \sqrt{\frac{-\beta}{8}} \xi \right) + \coth_{pq} \left( \sqrt{\frac{-\beta}{8}} \xi \right) \right) \right),$$

$$q_{1,9}(x, y, z, t) = \pm \sqrt{\frac{2L}{b}} \left( \sqrt{\frac{-\beta}{8}} \left( \tanh_{fg} \left( \sqrt{\frac{-\beta}{8}} \xi \right) + \coth_{pq} \left( \sqrt{\frac{-\beta}{8}} \xi \right) \right) \right)$$

$$\times e^{i(-\kappa_1 x - \kappa_2 y - \kappa_3 z - \sigma^2 t + \sigma W(t) + \omega t + \theta)}$$
(21)

Where  $\xi = B_1 x + B_2 y + B_3 z - Vt$ ,  $\beta = \frac{\sigma^2 + S - \omega}{r}$ .

**Case IV**: If  $\beta > 0$ , and  $\kappa = \frac{\beta^2}{4}$ , afterward:

$$P_{1,10}^{\pm} = \pm \sqrt{\frac{2L}{b}} \sqrt{\frac{\beta}{2}} tan_{fg} \left( \sqrt{\frac{\beta}{2}} \xi \right),$$

$$q_{1,10}(x, y, z, t) = \pm \sqrt{\frac{2L}{b}} \sqrt{\frac{\beta}{2}} tan_{fg} \left( \sqrt{\frac{\beta}{2}} \xi \right) \times e^{i(-\kappa_1 x - \kappa_2 y - \kappa_3 z - \sigma^2 t + \sigma W(t) + \omega t + \theta)},$$
(22)

$$\begin{split} P_{1,11}^{\pm} &= \pm \sqrt{\frac{2L}{b}} \sqrt{\frac{\beta}{2}} \cot_{fg} \left( \sqrt{\frac{\beta}{2}} \xi \right), \\ q_{1,11}(x,y,z,t) &= \pm \sqrt{\frac{2L}{b}} \sqrt{\frac{\beta}{2}} \cot_{fg} \left( \sqrt{\frac{\beta}{2}} \xi \right) \times e^{i(-\kappa_1 x - \kappa_2 y - \kappa_3 z - \sigma^2 t + \sigma W(t) + \omega t + \theta)}, \end{split} \tag{23}$$

$$P_{1,12}^{\pm} = \pm \sqrt{\frac{2L}{b}} \left( \sqrt{\frac{\beta}{2}} \left( tan_{fg} (\sqrt{2\beta} \, \xi) \pm \sqrt{fg} \, sec_{fg} (\sqrt{2\beta} \, \xi) \right) \right),$$

$$q_{1,12}(x, y, z, t) = \pm \sqrt{\frac{2L}{b}} \left( \sqrt{\frac{\beta}{2}} \left( tan_{fg} (\sqrt{2\beta} \, \xi) \pm \sqrt{fg} \, sec_{fg} (\sqrt{2\beta} \, \xi) \right) \right)$$

$$\times e^{i(-\kappa_1 x - \kappa_2 y - \kappa_3 z - \sigma^2 t + \sigma W(t) + \omega t + \theta)},$$
(24)

$$P_{1,13}^{\pm} = \pm \sqrt{\frac{2L}{b}} \left( \sqrt{\frac{\beta}{2}} \left( \cot_{fg} \left( \sqrt{2\beta} \, \xi \right) + \csc_{fg} \left( \sqrt{2\beta} \, \xi \right) \right) \right),$$

$$q_{1,13}(x, y, z, t) = \pm \sqrt{\frac{2L}{b}} \left( \sqrt{\frac{\beta}{2}} \left( \cot_{fg} \left( \sqrt{2\beta} \, \xi \right) + \csc_{fg} \left( \sqrt{2\beta} \, \xi \right) \right) \right)$$

$$\times e^{i(-\kappa_1 x - \kappa_2 y - \kappa_3 z - \sigma^2 t + \sigma W(t) + \omega t + \theta)},$$
(25)

$$P_{1,14}^{\pm} = \pm \sqrt{\frac{2L}{b}} \left( \sqrt{\frac{\beta}{8}} \left( tan_{fg} \left( \sqrt{\frac{\beta}{8}} \xi \right) + cot_{fg} \left( \sqrt{\frac{\beta}{8}} \xi \right) \right) \right),$$

$$q_{1,14}(x, y, z, t) = \pm \sqrt{\frac{2L}{b}} \left( \sqrt{\frac{\beta}{8}} \left( tan_{fg} \left( \sqrt{\frac{\beta}{8}} \xi \right) + cot_{fg} \left( \sqrt{\frac{\beta}{8}} \xi \right) \right) \right)$$

$$\times e^{i(-\kappa_1 x - \kappa_2 y - \kappa_3 z - \sigma^2 t + \sigma W(t) + \omega t + \theta)},$$

$$(26)$$

Where  $\xi = B_1 x + B_2 y + B_3 z - Vt$ ,  $\beta = \frac{\sigma^2 + S - \omega}{L}$ .

#### 4. Hamiltonian and Jacobian of the system

Critical points Let, P' = U then [28,29]

$$U' = -\frac{(\omega - \sigma^2 - S)}{L}P + \frac{b}{L}P^3,$$
(27)

Critical point U = 0 then

$$-\frac{(\omega - \sigma^2 - S)}{L}P + \frac{b}{L}P^3 = 0,$$

$$P\left(-\frac{(\omega - \sigma^2 - S)}{L} + \frac{b}{L}P^2\right) = 0$$

$$\Rightarrow P = 0, \quad P^2 = \frac{(\omega - \sigma^2 - S)}{b} \to P = \pm \sqrt{\frac{(\omega - \sigma^2 - S)}{b}},$$
(28)

Hence we get three critical points

$$(P,U) = (0,0), \quad \left(\sqrt{\frac{(\omega - \sigma^2 - S)}{b}}, 0\right), \left(-\sqrt{\frac{(\omega - \sigma^2 - S)}{b}}, 0\right). \tag{29}$$

Hamiltonian

$$H(P,U) = \frac{U^2}{2} - \frac{b}{4L}P^4 + \frac{(\omega - \sigma^2 - S)}{2L}P^2,$$
(30)

Let, F(P, U) = U then

$$G(P,U) = -\frac{(\omega - \sigma^2 - S)}{L}P + \frac{b}{L}P^3,$$
(31)

Jacobian:

$$J = \begin{vmatrix} \frac{\partial F}{\partial P} & \frac{\partial F}{\partial U} \\ \frac{\partial G}{\partial P} & \frac{\partial G}{\partial U} \end{vmatrix}$$

$$J = D(P, U) = \begin{vmatrix} 0 & 1 \\ -\frac{(\omega - \sigma^2 - S)}{L} + \frac{3b}{L}P^2 & 0 \end{vmatrix} = \frac{(\omega - \sigma^2 - S)}{L} + \frac{3b}{L}P^2,$$
(32)

Now

$$J(0,0) = \begin{vmatrix} 0 & 1 \\ -\frac{(\omega - \sigma^2 - S)}{L} & 0 \end{vmatrix} = \frac{(\omega - \sigma^2 - S)}{L},$$
(33)

And

$$J\left(\pm\sqrt{\frac{(\omega-\sigma^2-S)}{b}},0\right) = \begin{vmatrix} 0 & 1 \\ 2(\omega-\sigma^2-S) & 0 \end{vmatrix} = -\frac{2(\omega-\sigma^2-S)}{L}.$$
 (34)

### 5. Analyzing bifurcation

V. if D(P, U) < 0, then (P, U) is a saddle point;

VI. if D(P, U) > 0, then (P, U) is a center point;

VII. if D(P, U) = 0, then (P, U) is a cuspidal point.

Here are possible outcomes resulting from varying the parameters involved.

Case 1: 
$$\frac{(\omega - \sigma^2 - S)}{L} < 0$$
 and  $\frac{b}{L} < 0$ 

By choosing a parameter regime as  $B_1 = 0.9$ ,  $B_2 = 0.8$ ,  $B_3 = 0.7$ ,  $B_3 = 0.8$ ,  $B_4 = 0.8$ ,  $B_5 = 0.8$ ,  $B_6 = 0.$ 

Case 2: 
$$\frac{(\omega - \sigma^2 - S)}{L} < 0$$
 and  $\frac{b}{L} > 0$ 

By selecting a parameter regime as  $B_1 = 0.9$ ,  $B_2 = 0.8$ ,  $B_3 = 0.7$ ,  $A_1 = 0.8$ ,  $A_2 = 0.75$ ,  $A_3 = 0.9$ ,  $A_4 = 0.75$ ,  $A_5 = 1$ ,  $A_6 = 1.9$ ,  $A_1 = 0.9$ ,  $A_2 = 0.67$ ,  $A_3 = 0.7$ ,  $A_4 = 0.9$ ,  $A_5 = 0.9$ ,  $A_6 = 0.9$ ,  $A_6 = 0.9$ ,  $A_7 = 0.9$ ,  $A_8 = 0.9$ ,  $A_9 =$ 

Case 3: 
$$\frac{(\omega - \sigma^2 - S)}{L} > 0$$
 and  $\frac{b}{L} < 0$ 

By selecting a parameter regime as  $B_1 = 0.9$ ,  $B_2 = 0.8$ ,  $B_3 = 0.7$ ,  $A_1 = 0.8$ ,  $A_2 = 0.75$ ,  $A_3 = 0.9$ ,  $A_4 = 0.75$ ,  $A_5 = 1$ ,  $A_6 = 1.9$ ,  $A_1 = 0.9$ ,  $A_2 = 0.67$ ,  $A_3 = 0.7$ ,  $A_4 = 0.7$ ,  $A_5 = 0.7$ ,  $A_6 = 0.7$ ,  $A_6 = 0.7$ ,  $A_6 = 0.7$ ,  $A_6 = 0.7$ ,  $A_7 = 0.7$ ,  $A_8 = 0.7$ ,  $A_9 =$ 

Case4: 
$$\frac{(\omega - \sigma^2 - S)}{L} > 0$$
 and  $\frac{b}{L} > 0$ 

By selecting a parameter regime as  $B_1 = 0.9$ ,  $B_2 = 0.8$ ,  $B_3 = 0.7$ ,  $A_1 = 0.8$ ,  $A_2 = 0.75$ ,  $A_3 = 0.9$ ,  $A_4 = 0.75$ ,  $A_5 = 1$ ,  $A_6 = 1.9$ ,  $A_6 = 1$ 

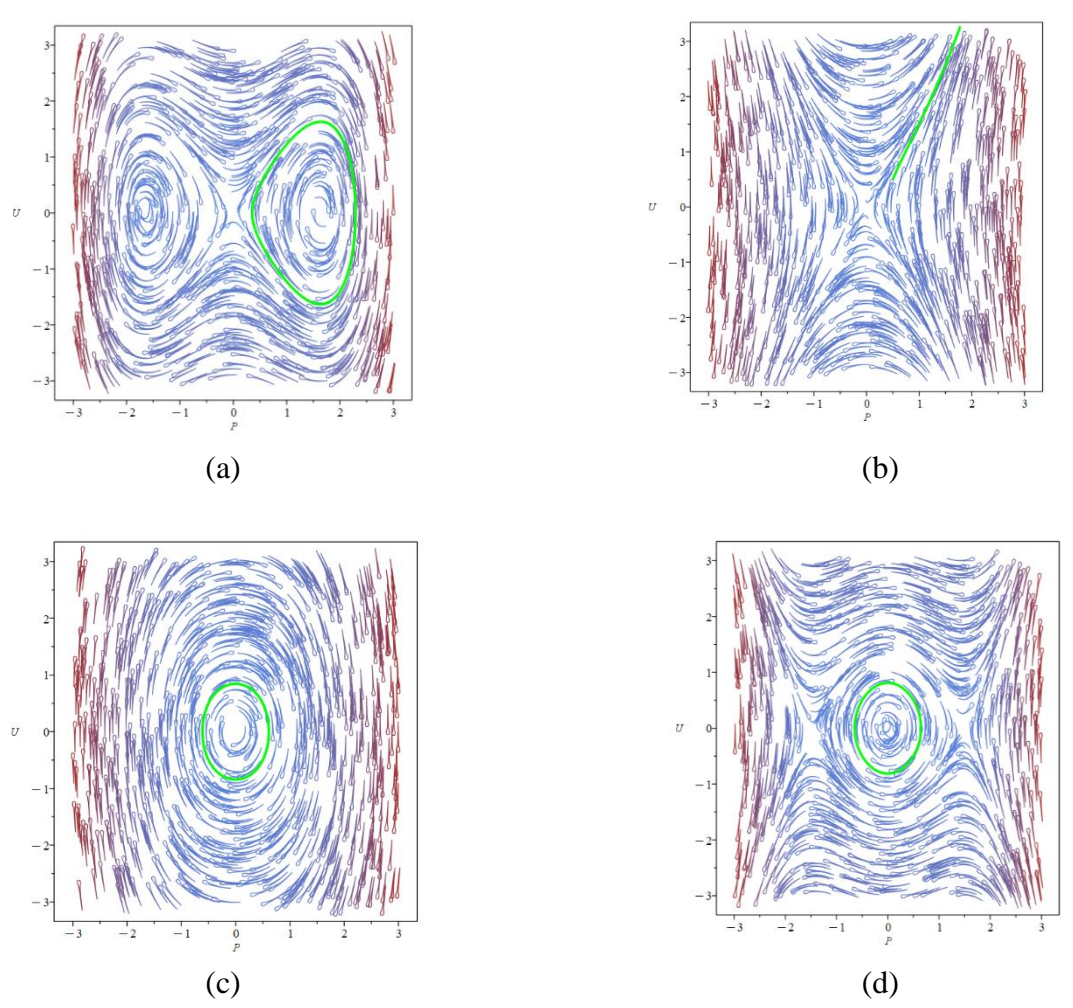


Figure 1. phase portraits of the planar system(20) when  $\mathbf{a} = \frac{(\omega - \sigma^2 - S)}{L} < 0$  and  $\frac{b}{L} < 0$ ,  $\mathbf{b} = \frac{(\omega - \sigma^2 - S)}{L} < 0$  and  $\frac{b}{L} > 0$ ,  $\mathbf{c} = \frac{(\omega - \sigma^2 - S)}{L} > 0$  and  $\frac{b}{L} > 0$ .

#### 6. Chaotic behaviors

In this subsection, by considering a perturbed term in the resulting planar system, the existence of chaotic behaviors investigated by analyzing some two-dimension all phase portraits.to start, consider the following planar system

$$\begin{cases}
\frac{dP(t)}{dt} = U(t), \\
\frac{dU(t)}{dt} = -\frac{(\omega - \sigma^2 - S)}{L}P(t) + \frac{b}{L}P^3(t) + A\cos(Bt),
\end{cases}$$
(35)

Invoving the perturbed term A cos (Bt) , where A and B signify the amplitude and frequency of the system, respectively .In Fig.2, two dimensional phase portraits of *the* wang equation (35),  $B_1 = 0.9$ ,  $B_2 = 0.8$ ,  $B_3 = 0.7$ ,  $a_1 = 0.8$ ,  $a_2 = 0.75$ ,  $a_3 = 0.9$ ,  $a_4 = 0.75$ ,  $a_5 = 1$ ,  $a_6 = 1.9$ ,  $a_6 = 1.9$ ,  $a_8 = 0.9$ ,  $a_8 = 0$ 

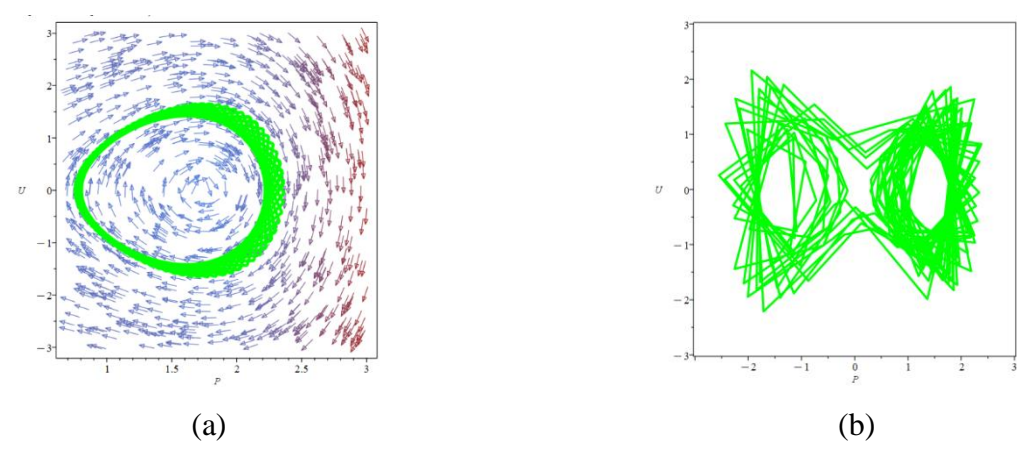


Figure 2. two - dimensional phase portraits of the wang equation (28),  $B_1 = 0.9$ ,  $B_2 = 0.8$ ,  $B_3 = 0.7$ ,  $a_1 = 0.8$ ,  $a_2 = 0.75$ ,  $a_3 = 0.9$ ,  $a_4 = 0.75$ ,  $a_5 = 1$ ,  $a_6 = 1.9$ ,  $\kappa_1 = 0.9$ ,  $\kappa_2 = 0.67$ ,  $\kappa_3 = 0.7$ ,  $\omega = 0.9$ ,  $\sigma = 0$ , b = 0.6 and A = 0.5 when  $a_1 = 0.5$  when  $a_2 = 0.75$ .

# 7. Sensitivity Analysis

In this subsection, the sensitivity analysis of the planar system (27) is accomplished using the Runge -Kutta method. To this end, the following planar system

$$\begin{cases} \frac{dP(t)}{dt} = U(t), \\ \frac{dU(t)}{dt} = -\frac{(\omega - \sigma^2 - S)}{L} P(t) + \frac{b}{L} P^3(t), \end{cases}$$
(36)

Is solved by the Runge \_Kutta method for  $B_1=0.9, B_2=0.8, B_3=0.7, a_1=0.8$  ,  $a_2=0.75, a_3=0.9, a_4=0.75, a_5=1, a_6=1.9, \kappa_1=0.9$  ,  $\kappa_2=0.67, \kappa_3=0.7$ 

,  $\omega = 0.9$ ,  $\sigma = 0$ , and b = 0.6 when the initial conditions are  $a \neq 0.0$  are  $a \neq 0.0$  and  $a \neq 0.0$  and  $a \neq 0.0$  and  $a \neq 0.0$  and  $a \neq 0.0$  are  $a \neq 0.0$  and  $a \neq 0.0$  and  $a \neq 0.0$  are  $a \neq 0.0$  are  $a \neq 0.0$  and  $a \neq 0.0$  are  $a \neq 0.0$  are  $a \neq 0.0$  and  $a \neq 0.0$  are  $a \neq 0.0$  and  $a \neq 0.0$  are  $a \neq 0.0$  are  $a \neq 0.0$  and  $a \neq 0.0$  are  $a \neq 0.0$  are  $a \neq 0.0$  and  $a \neq 0.0$  are  $a \neq 0.0$  are  $a \neq 0.0$  and  $a \neq 0.0$  are  $a \neq 0.0$  are  $a \neq 0.0$  and  $a \neq 0.0$  are  $a \neq 0.0$  and  $a \neq 0.0$  are  $a \neq 0.0$  are  $a \neq 0.0$  and  $a \neq 0.0$  are  $a \neq 0.0$  and  $a \neq 0.0$  are  $a \neq 0.0$  are  $a \neq 0.0$  and  $a \neq 0.0$  are  $a \neq 0.0$  and  $a \neq 0.0$  are  $a \neq 0.0$  are  $a \neq 0.0$  and  $a \neq 0.0$  are  $a \neq 0.0$  are  $a \neq 0.0$  and  $a \neq 0.0$  are  $a \neq 0.0$  are  $a \neq 0.0$  and  $a \neq 0.0$  are  $a \neq 0.0$  and  $a \neq 0.0$  are  $a \neq 0.0$  are  $a \neq 0.0$  are  $a \neq 0.0$  are  $a \neq 0.0$  and  $a \neq 0.0$  are  $a \neq 0.0$  are a

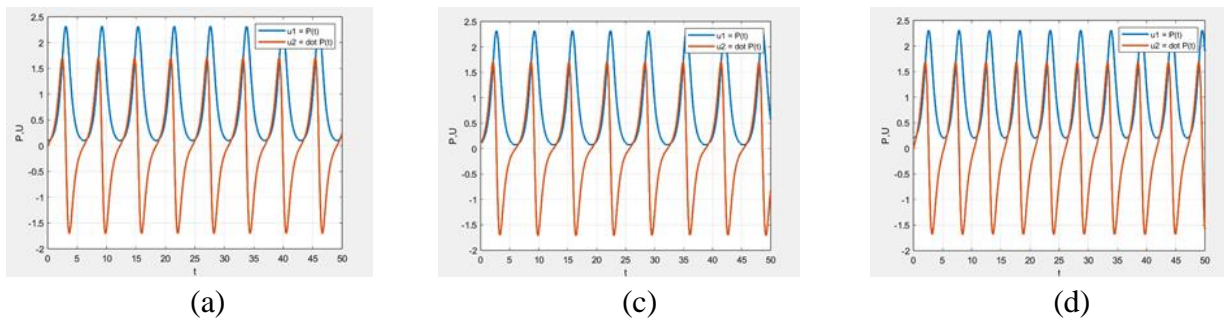


Figure 3. Sensitive analysis of the wang Eq. (36) for  $B_1 = 0.9$ ,  $B_2 = 0.8$ ,  $B_3 = 0.7$ ,  $a_1 = 0.8$ ,  $a_2 = 0.75$ ,  $a_3 = 0.9$ ,  $a_4 = 0.75$ ,  $a_5 = 1$ ,  $a_6 = 1.9$ ,  $κ_1 = 0.9$ ,  $κ_2 = 0.67$ ,  $κ_3 = 0.7$ , ω = 0.9, σ = 0, and σ = 0.6 when the initial conditions are (a) σ = 0.1 and σ = 0.1 and

*Figure 3* shows the results given by such an effective scheme. looking at the figures, it is clear that small changes in the initial conditions do not affect the stability of the solution very much.

#### 8. Soliton solutions

$$P'' = -\frac{(\omega - \sigma^2 - S)}{L}P + \frac{b}{L}P^3,\tag{37}$$

From (37), we establish a planar system as:

$$\begin{cases} \frac{dP(\xi)}{d\xi} = U(\xi), \\ \frac{dU(\xi)}{d\xi} = -\frac{(\omega - \sigma^2 - S)}{L} P(\xi) + \frac{b}{L} P^3(\xi), \end{cases}$$
(38)

The system (38) is a Hamiltonian system with the following Hamiltonian function:

$$H(P,U) = \frac{U^2}{2} + \frac{(\omega - \sigma^2 - S)}{2L} P^2(\xi) - \frac{b}{4L} P^4(\xi) = h,$$
(39)

where h is Hamiltonian. Thus, we have

$$\frac{U^{2}}{2} = h - \frac{(\omega - \sigma^{2} - S)}{2L} P^{2} + \frac{b}{4L} P^{4}, 
\Rightarrow U = \pm \sqrt{2} \sqrt{h - \frac{(\omega - \sigma^{2} - S)}{2L} P^{2} + \frac{b}{4L} P^{4},} \tag{40}$$

Now,

$$\frac{dP}{\pm\sqrt{2}\sqrt{h-\frac{(\omega-\sigma^2-S)}{2L}P^2+\frac{b}{4L}P^4}} = d\xi$$

$$\Rightarrow \int \frac{dP}{\sqrt{h-\frac{(\omega-\sigma^2-S)}{2L}P^2+\frac{b}{4L}P^4}} = \pm\sqrt{2}(\xi+\xi_0).$$

Let h = 0, then, Eq. (1) has the bright soliton solution as the follows [25]:

$$q_{1,15}(x,y,z,t) = \pm \sqrt{\frac{2(\omega - \sigma^2 - S)}{b}} \operatorname{sech}\left(\sqrt{\frac{-\omega + \sigma^2 + S}{L}} \left(B_1 x + B_2 y + B_3 z - Vt + \xi_0\right)\right) \times e^{i(-\kappa_1 x - \kappa_2 y - \kappa_3 z - \sigma^2 t + \sigma W(t) + \omega t + \theta)}.$$
(41)

With constraints

$$(-\omega + \sigma^2 + S)L > 0, (42)$$

$$(\omega - \sigma^2 - S) b > 0, \tag{43}$$

$$L = a_1 B_1^2 + a_2 B_2^2 + a_3 B_3^2 + 2a_4 B_1 B_2 - 2a_5 B_1 B_3 - 2a_6 B_2 B_3,$$

$$S = a_1 \kappa_1^2 + a_2 \kappa_2^2 + a_3 \kappa_3^2 + 2a_4 \kappa_1 \kappa_2 - 2a_5 \kappa_1 \kappa_3 - 2a_6 \kappa_2 \kappa_3.$$

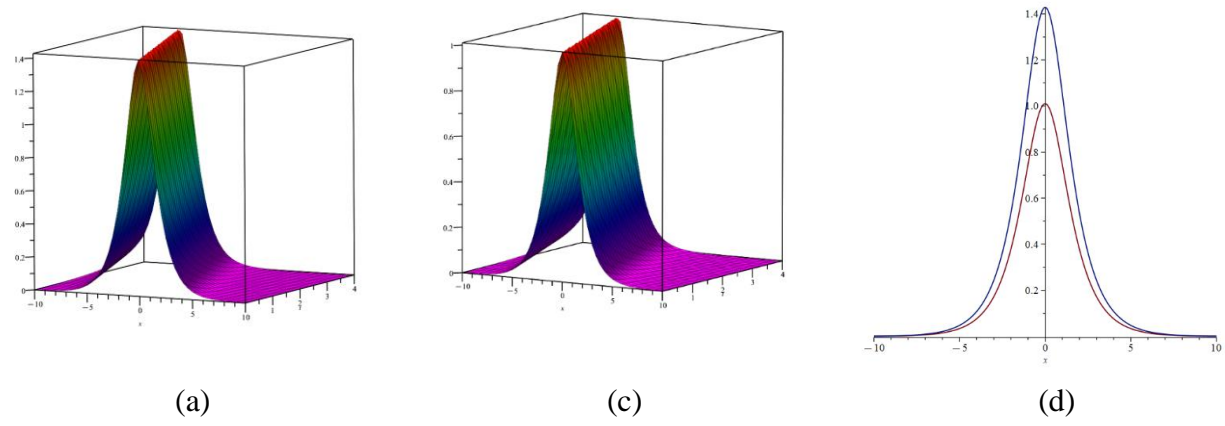


Figure 4. Bright soliton for  $B_1 = 0.9$ ,  $B_2 = 0.8$ ,  $B_3 = 0.7$ ,  $a_1 = 0.8$ ,  $a_2 = 0.75$ ,  $a_3 = 0.9$ ,  $a_4 = 0.75$ ,  $a_5 = 1$ ,  $a_6 = 1.9$ ,  $\kappa_1 = 0.9$ ,  $\kappa_2 = 0.67$ ,  $\kappa_3 = 0.7$ ,  $\omega = 0.9$ ,  $\sigma = 1$   $\xi_0 = 0$ ,  $\theta = 0.9$ , W = 0, and y = z = 0 when  $\mathbf{a}$  b = 0.6;  $\mathbf{c}$  b = 1.2;  $\mathbf{d}$  t = 0, b = 0.6, and t = 0, b = 1.2.

Let  $h = \frac{(\omega - \sigma 2 - S)^2}{4hL}$ , then, Eq. (1) has the dark soliton solution as the follows [25]:

$$q_{1,16}(x,y,z,t) = \pm \sqrt{\frac{(\omega - \sigma^2 - S)}{b}} \tanh \left( \sqrt{\frac{(\omega - \sigma^2 - S)}{2L}} \left( B_1 x + B_2 y + B_3 z - Vt + \xi_0 \right) \right)$$

$$\times e^{i(-\kappa_1 x - \kappa_2 y - \kappa_3 z - \sigma^2 t + \sigma W(t) + \omega t + \theta)}$$
(44)

$$(\omega - \sigma^2 - S) L > 0, \tag{45}$$

$$(\omega - \sigma^2 - S) b > 0, \tag{46}$$

$$L = a_1 B_1^2 + a_2 B_2^2 + a_3 B_3^2 + 2a_4 B_1 B_2 - 2a_5 B_1 B_3 - 2a_6 B_2 B_3,$$

$$S = a_1 \kappa_1^2 + a_2 \kappa_2^2 + a_3 \kappa_3^2 + 2a_4 \kappa_1 \kappa_2 - 2a_5 \kappa_1 \kappa_3 - 2a_6 \kappa_2 \kappa_3.$$

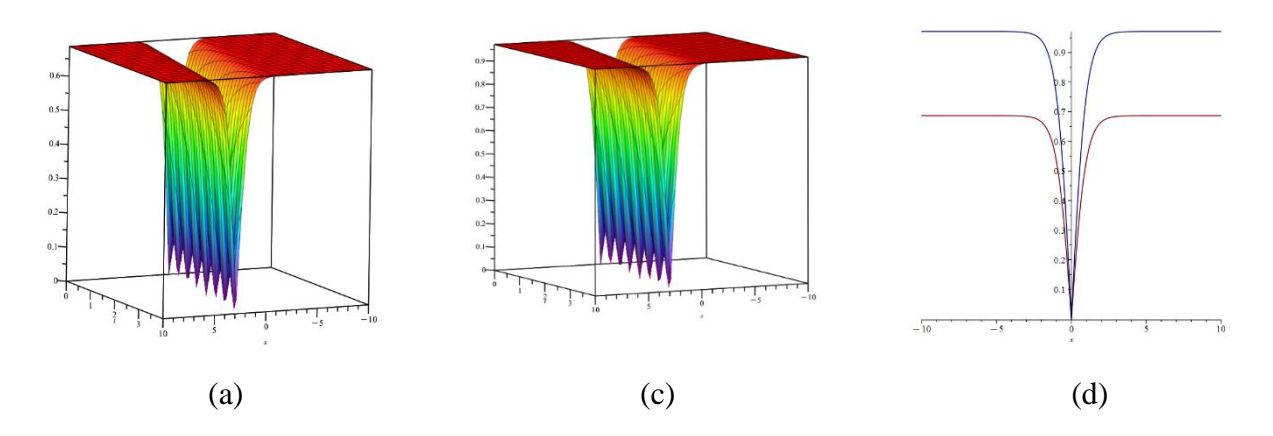


Figure 5. dark soliton for  $B_1=0.9$ ,  $B_2=0.85$ ,  $B_3=0.7$ ,  $a_1=1.4$ ,  $a_2=0.8$ ,  $a_3=0.9$ ,  $a_4=0.8$ ,  $a_5=1$ ,  $a_6=1.6$ ,  $\kappa_1=0.9$ ,  $\kappa_2=0.7$ ,  $\kappa_3=0.6$ ,  $\omega=2$ ,  $\sigma=1$   $\xi_0=0$ ,  $\theta=0.9$ , W=0, and y=z=0 when a b=0.6, c b=1.2, d t=0, b=0.6, and t=0, b=1.2.

To show the effect of the Kerr nonlinearity on the wave characteristics of bright and dark soliton , we first plot the bright soliton in Fig.4 for  $B_1=0.9$ ,  $B_2=0.8$ ,  $B_3=0.7$ ,  $a_1=0.8$ ,  $a_2=0.75$ ,  $a_3=0.9$ ,  $a_4=0.75$ ,  $a_5=1$ ,  $a_6=1.9$ ,  $\kappa_1=0.9$ ,  $\kappa_2=0.67$ ,  $\kappa_3=0.7$ ,  $\omega=0.9$ ,  $\sigma=1$ , W=0,  $\xi_0=0$ , and y=z=0,  $\theta=0.9$ , when (a) b=0.6; (c) b=1.2. From these figures, it can be concluded that the width and height of the bright soliton decrease by increasing the coefficient of the Kerr nonlinearity .Additionally we depict the dark soliton in Fig.5 for as  $B_1=0.9$ ,  $B_2=0.85$ ,  $B_3=0.7$ ,  $a_1=1.4$ ,  $a_2=0.8$ ,  $a_3=0.9$ ,  $a_4=0.8$ ,  $a_5=1$ ,  $a_6=1.6$ ,  $\kappa_1=0.9$ ,  $\kappa_2=0.7$ ,  $\kappa_3=0.6$ ,  $\omega=2$ ,  $\sigma=1$ , w=0,  $\xi=0$ , and z=0, z=0,

#### 9. Conclusions

The application of SSM to the extended (3+1)-dimensional stochastic nonlinear Schrödinger equation in terms of multiplicative noise has provided valuable knowledge into the dynamics of complex nonlinear equations and derived a range of exact solutions, including soliton-like, periodic, bright, dark, and singular solutions. We uncovered critical transition points where the system's behavior changes significantly, the bifurcation analysis is conducted which highlighted the complex nature of nonlinear dynamics. The addition of external periodic function enhanced the study of chaotic behaviors and reveal areas of instability that show the unpredictable nature of such systems. Sensitivity analysis further focused how small changes in system parameters could yield to dramatic changes in the dynamics, offering insights into the robustness and responsiveness of the approach. The stability of equilibrium points was analyzed by linearizing the system which allow us to find the nature of these points and their influence on long-term behavior.

## References

[1] S. Sadiq &, A. Javid; Novel solitary wave solutions in dual-mode simplified modified Camassa–Holm equation in shallow water waves. *Opt. Quantum Electron.* 56(3), (2024), 1–13.

- [2] M.Bilal, J. Ren, M. Inc, & R. T. Alqahtani. Dynamics of solitons and weakly ion-acoustic wave structures to the nonlinear dynamical model via analytical techniques. *Opt. Quantum Electron.* 55(7), (2023), 656.
- [3] M.Bilal, J. Ren. Dynamics of exact solitary wave solutions to the conformable time-space fractional model with reliable analytical approaches. *Opt. Quantum Electron.* 54(1), (2022), 40.
- [4] M.Bilal, & J. Ahmad. Dispersive solitary wave solutions for the dynamical soliton model by three versatile analytical mathematical methods. *Eur. Phys. J. Plus* 137(6), (2022), 674.
- [5] M. Bilal, H. Wencheng, & J. Ren. Different wave structures to the Chen–Lee–Liu equation of monomode fibers and its modulation instability analysis. *Eur. Phys. J. Plus* 136, (2021). 1–15.
- [6] M. Z. Baber, N. Ahmed, C. Xu, M. S. Iqbal, and T. Sulaiman . A computational scheme and its comparison with optical soliton solutions for the stochastic Chen–Lee–Liu equation with sensitivity analysis. Mod. Phys. Lett. B, (2024), 2450376.
- [7] C. Xu. Insights into COVID-19 stochastic modelling with effects of various transmission rates: Simulations with real statistical data from UK, Australia, Spain, and India. *Physica Scripta* 99(2), (2024), 025218.
- [8] H. U. Rehman, A. U. Awan, S. M. Eldin, & I. Iqbal. Study of optical stochastic solitons of Biswas-Arshed equation with multiplicative noise. *AIMS Math.*, 8(9), . (2023), 21606-21621.
- [9] H. U. Rehman, I. Iqbal, H. Zulfiqar, D. Gholami, H. Rezazadeh. "Stochastic soliton solutions of conformable nonlinear stochastic systems processed with multiplicative noise." Phys. Lett. A 486, (2023), 129100.
- [10] N. Bruti-Liberati. "Numerical solution of stochastic differential equations with jumps in finance." Ph.D. diss. (2007).
- [11] S. Sun, X. Zhang. "Asymptotic behavior of a stochastic delayed chemostat model with nutrient storage." J. Biol. Syst. 26(02), (2018), 225–246.
- [12] W. W. Mohammed, C. Cesarano. "The soliton solutions for the (4+1)-dimensional stochastic Fokas equation." Math. Methods Appl. Sci. 46(6), (2023), 7589-7597.
- [13] W. W. Mohammed, F. M. Al-Askar, C. Cesarano. "The analytical solutions of the stochastic mKdV equation via the mapping method." Mathematics 10(22), (2022), 4212.
- [14] H. U. Rehman, N. Ullah, M. Imran. "Optical solitons of Biswas-Arshed equation in birefringent fibers using extended direct algebraic method." Optik 226, (2021), 165378.
- [15] H. U. Rehman, N. Ullah, M. Imran. "Highly dispersive optical solitons using Kudryashov's method." Optik 199, (2019), 163349.
- [16] H. U. Rehman, M. S. Saleem, M. Zubair, S. Jafar, I. Latif. "Optical solitons with Biswas-Arshed model using mapping method." Optik 194, (2019), 163091.
- [17] A. Kurt, A. Tozar, O. Tasbozan. "Applying the new extended direct algebraic method to solve the equation of obliquely interacting waves in shallow waters." J. Ocean Univ. China 19, (2020), 772.
- [18] P. N. Ryabov, D. I. Sinelshchikov, M. B. Kochanov. "Application of the Kudryashov method for finding exact solutions of the high-order nonlinear evolution equations." Appl. Math. Comput. 218(7), (2011), 3965-3972.
- [19] D. Shi, H. U. Rehman, I. Iqbal, M. Vivas-Cortez, M. S. Saleem, X. Zhang. "Analytical study of the dynamics in the double-chain model of DNA." (2023).
- [20] H. U. Rehman, A. U. Awan, E. M. Tag-ElDin, S. E. Alhazmi, M. F. Yassen, R. Haider. "Extended hyperbolic function method for the (2+1)-dimensional nonlinear soliton equation." Results Phys. 40, (2022), 105802.
- [21] N. Ullah, M. I. Asjad, T. Muhammad, A. Akgul. "Analysis of power law non-linearity in solitonic solutions using extended hyperbolic function method." (2023).
- [22] Z. Hong, H. Ji-Guang, W. Wei-Tao, A. Hong-Yong. "Applications of extended hyperbolic function method for quintic discrete nonlinear Schrödinger equation." Commun. Theor. Phys. 47(3), (2007), 474.
- [23] H. U. Rehman, M. A. Imran, N. Ullah, A. Akgul. "Exact solutions of (2+1)-dimensional Schrödinger's hyperbolic equation using different techniques." Numer. Methods Partial Differ. Equations. (2023).
- [24]G. Wang. "A new (3+1)-dimensional Schrodinger equation: derivation, soliton solutions and conservation laws". Nonlinear Dyn. 104, (2021), 1595-1602
- [25] M. Mirzazadeh; A. Biswas; Y. Yildirim & S. Saravana Veni. "Optical bullets with cross-spatio dispersion and multiplicative white noise". Journal of Optics. Submitted.

- [26] H. U. Rehman, I. Iqbal, S. Subhi Aiadi, N. Mlaiki, M. S. Saleem. "Soliton solutions of Klein-Fock-Gordon equation using Sardar subequation method." Mathematics 10(18), (2022), 3377.
- [27] Sadia Yasin · Asif Khan · Shabir Ahmad · M. S. Osman. New exact solutions of (3+1)-dimensional modified KdV -Zakharov-Kuznetsov equation by Sardar-subequation method. December 2023
- [28] A. Refaie Ali, H. Or Roshid, S. Islam & A. Khatun. "Analyzing bifurcation, stability, and wave solutions in nonlinear telecommunications models using transmission lines, Hamiltonian and Jacobian techniques". Scientific Reports. 14 (1), (2024), 15282.
- [29] K. Hosseini, E. Hinal & M. Ilie. "Bifurcation analysis, chaotic behaviors, sensitivity analysis, and soliton solutions of a generalized Schrodinger equation". Nonlinear Dynamics. 111 (18), (2024), 17455-17462.
- [30] N. Taghizadeh, M. Mirzazadeh & F. Farahrooz. "Exact solutions of the nonlinear Schrodinger equation by the first integral method". Journal of Mathematical Analysis and Applications. 374(2), (2011), 549-553.
- [31] H.U. Rehman, I. Iqbal, M. Mirzazadeh, M.S. Hashemi, A.U. Awan & A.M. Hassan. "Optical solitons of new extended (3+1)-dimensional nonlinear Kudryashov's equation via φ 6 -model expansion method". Optical and Quantum Electronics. 56 (3), (2024), 279.